# Photofield-Effect in Amorphous In-Ga-Zn-O (a-IGZO) Thin-Film Transistors

**Tze-Ching Fung[a], Chiao-Shun Chuang[c], Kenji Nomura[b], Han-Ping David Shieh[c], Hideo Hosono[b], and Jerzy Kanicki[a]**

**Abstract**

We studied both the wavelength and intensity dependent photo-responses (photofield-effect) in amorphous In-Ga-Zn-O (a-IGZO) thin-film transistors (TFTs). During the a-IGZO TFT illumination with the wavelength range from 460~660 nm (visible range), the off-state drain current ($I_{DS\_off}$) only slightly increased while a large increase was observed for the wavelength below 400 nm. The observed results are consistent with the optical gap of ~3.05eV extracted from the absorption measurement. The a-IGZO TFT properties under monochromatic illumination ($\lambda$=420nm) with different intensity was also investigated and $I_{DS\_off}$ was found to increase with the light intensity. Throughout the study, the field-effect mobility ($\mu_{eff}$) is almost unchanged. But due to photo-generated charge trapping, a negative threshold voltage ($V_{th}$) shift is observed. The mathematical analysis of the photofield-effect suggests that a highly efficient UV photocurrent conversion process in TFT off-region takes place. Finally, a-IGZO mid-gap density-of-states (DOS) was extracted and is more than an order of magnitude lower than reported value for hydrogenated amorphous silicon (a-Si:H), which can explain a good switching properties observed for a-IGZO TFTs.

**Keywords** : Metal oxide semiconductor, InGaZnO, TFT, Photofield effect

## 1. Introduction

Conventional active-matrix (AM) flat panel displays (FPDs) are based on amorphous or polycrystalline silicon thin-film transistor (TFT) technology. As a great advantage, hydrogenated amorphous silicon (a-Si:H) thin film can be uniformly deposited on to the glass substrate over large area by plasma enhanced chemical vapor deposition (PECVD) system [1]. Nonetheless, the main limitations of the a-Si:H are electrical instability and a low (usually < 1 $cm^2/Vs$) field-effect mobility ($\mu_{eff}$), which reduces the pixel aperture ratio and driving ability for some demanding display applications [2]. Although poly-crystalline silicon TFT has a larger mobility (~100 $cm^2/Vs$), due to the need of re-crystallization (such as excimer-laser annealing, ELA [3]), its electrical properties uniformity over a large area is not always acceptable for a high yield low cost manufacturing and high resolution display applications [2].

Because the next generation AM-FPDs [4] and flat panel photo-imagers [5] will pose a more stringent requirements, which cannot be handled by existing a-Si:H or poly-Si TFT backplane technology, such as low temperature deposition over large area, reduced pixel size (resolution), large dynamic range and high operational speed, there is an increasing demand among others for a new semiconductor material to overcome the above mentioned difficulties. Since year 2000, there has been great interest in adapting TFT made of transparent metal oxide semiconductors to future FPDs. Specifically, the ternary oxide system which consists of $In_2O_3$, $Ga_2O_3$ and ZnO has shown promising performance for TFT active layer with a high mobility (3~12 $cm^2/Vs$), low off-current (~$10^{-12}$A) and expected good uniformity over large area [6,7]. Today, amorphous In-Ga-Zn-O (a-IGZO) TFT has been successfully implemented in applications such as active-matrix organic light-emitting display (AM-OLED) [8], active-matrix liquid crystal display (AM-LCD) [9], electronic paper [10] and transparent

Manuscript received November 13, 2008; accepted for publication December 15, 2008.
Two of the authors (T.C. Fung and J. Kanicki) would like to thank DARPA HARDI Program (Dr. Devanand Shenoy) for their financial support during this work.
This paper received Award in Fundamental and Original Technology from The Minister of Education, Science and Technology of Republic of Korea during 8th International Meeting on Information Display (IMID) 2008.
Corresponding Author: Jerzy Kanicki
[a]Department of Electrical Engineering and Computer Science, University of Michigan, 1301 Beal Ave. Ann Arbor, Michigan 48109-2122, USA
[b]ERATO-SORST, JST, in Frontier Collaborative Research Center / Material and Structure Lab., Tokyo Institute of Technology, Yokohama 226-8503, Japan
[c]Department of Photonics & Display Institute, National Chiao Tung University, Hsinchu, 30010, Taiwan
**E-mail**: kanicki@eecs.umich.edu
**Tel**: 001-734-936-0964 **Fax**: 001-734-615-2843

electronics [7,11]. Since many of the proposed uses of the a-IGZO TFT will involve a possible exposure of device to backlight or ambient light during operation, it is very important to evaluate the a-IGZO TFT properties under illumination. In this paper, we investigate the wavelength and intensity dependent photo-responses (photofield-effect) in a-IGZO TFTs which are suitable for AM-FPD and active-matrix array detectors. We also presented, for the first time, the photofield-effect analysis of the a-IGZO TFT under UV-monochromatic photo illumination that was used for extraction of the a-IGZO density-of-states (DOS).

## 2. Experimental

Fig. 1 shows the cross-section and top view of the bottom gate a-IGZO TFT used in this study. A heavily P-doped ($n^{++}$) silicon wafer with 100 nm thermal oxide layer was used as the gate electrode and gate insulator, respectively. A 40 nm thick a-IGZO (In:Ga:Zn=1:1:1) active layer was deposited on the substrate by pulse-laser deposition (PLD) [12] and the deposition was done in an oxygen atmosphere without any intentional substrate heating. Before the source/drain metal electrodes deposition, a macro-island of a-IGZO was formed by edge-dipping/etching of the substrate in 0.1M HCl solution. The 50 nm thick aluminum (Al) source/drain electrodes were deposited through stencil mask openings by thermal evaporation. Finally, the device was thermally annealed in air at $300^0$C for 5 minutes. We also deposited a-IGZO thin film directly onto quartz substrate to measure its optical properties. The absorption spectrum of the a-IGZO thin-film was collected by a Cary 5E UV-VIS spectrometer using polarized light [13]. Quartz substrates were used to minimize the back ground interference during transmittance measurement.

Electrical measurement of the a-IGZO TFT were carried out with a probe station system located in a light tight box. The transistor electrical properties were measured by a PC controlled Agilent 4156 semiconductor parametric analyzer. During photofield effect measurement, photo excitation was provided by a Hg-Xe lamp in combination with

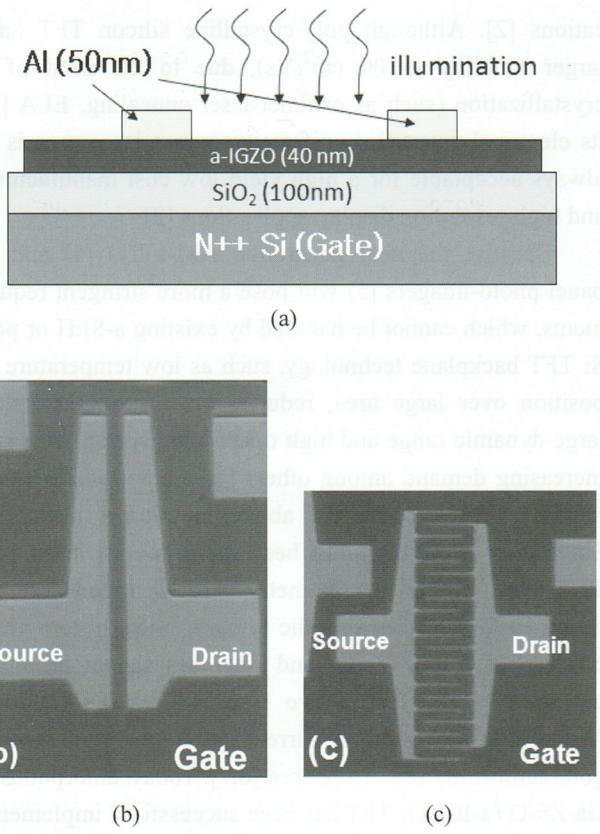


**Fig. 1.** (a) Cross-section of the PLD a-IGZO TFT device used in this study. (b) and (c) are die photos of regular and finger type (interdigitated) TFTs, respectively.

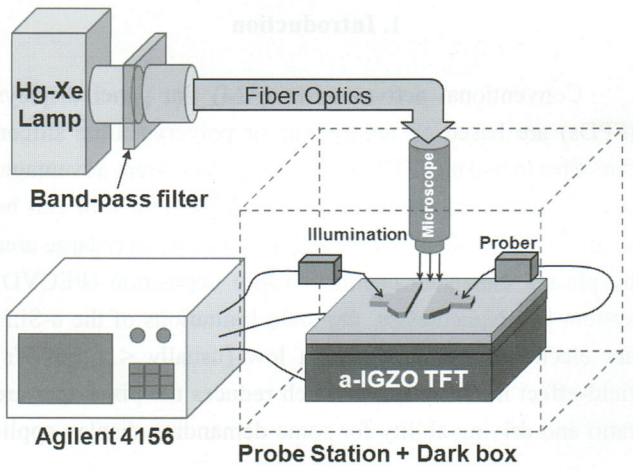


**Fig. 2.** The schematic of experimental setup used in this study. (From [20].)

**Table 1.** Experimental Conditions for Photofield-Effect Study

| Experimental Type | Wavelength (λ) | Photon Flux / Light Intensity (Irradiance) |
|---|---|---|
| Wavelength Dependent | 660nm ~ 365nm | $1\times10^{13}$ photons/cm$^2$s |
| Intensity Dependent | 420nm | Dark ~ 10μW/cm$^2$ |

narrow band filters and an optical fiber. The monochromic light passed through a fiber cable and probe station microscope, which is used to focus the illumination on the a-IGZO TFT channel. Fig. 2 shows the schematic of experimental setup used in this study. All measurements were done at room temperature in ambient air. Table 1 further lists the details of experimental conditions. It should be noticed that before each measurement the light intensity was calibrated by Oriel 70260 radiant power meter with the photodiode sensor attached. Each measurement step takes about 10 mins to achieve a steady state under illumination. Both regular and finger (interdigitated) types of TFTs were measured under illumination and show very similar photo-responses.

## 3. Result and Discussion

### *3.1 Optical Properties*

Fig. 3 shows the optical absorption spectrum of the PLD a-IGZO thin films (thickness=181nm). The absorption coefficient (α) of a-Si:H collected from other group [14] is also shown as a reference. The α of a-IGZO is at least an order of magnitude lower than it's a-Si:H counterpart within the investigated photon energy range. For example, for visible light (1.8~3.1eV), the α of a-Si:H is ranging from 3000 to ~$5\times10^5$ $cm^{-1}$ while α of a-IGZO is well below $10^3 cm^{-1}$ except the near UV region (~3.1eV). We assumed parabolic densities of band states within a-IGZO and extracted the optical energy band gap ($E_g$, also called Tauc gap) by applying the Tauc method [15]:

$$(\hbar\omega\alpha)^{1/2} = B(\hbar\omega - E_g) \quad (1)$$

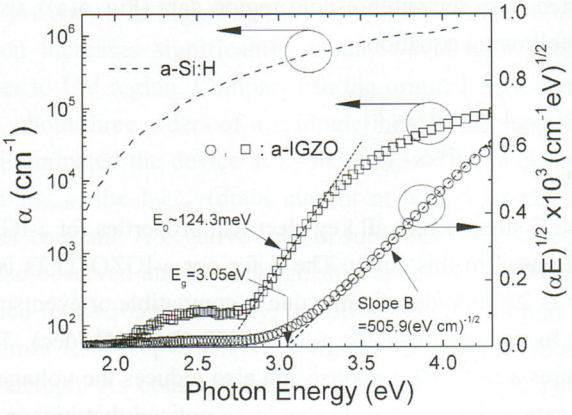


**Fig. 3.** Optical absorption spectrum of PLD a-IGZO (○, □) [28] and a-Si:H (dash line) [14] thin film.

where $\hbar\omega$ is the photon energy (E) and α is the absorption coefficient. The Tauc gap ($E_g$) was determined to be ~3.05 eV (and B=505.9 $(eV\text{-}cm)^{-1/2}$) as shown in Fig. 3. The result suggests that a high visible light transparency of the a-IGZO is due to its wide optical band-gap. We also observed the exponential optical energy dependence of the absorption coefficient in the vicinity of $E_g$ which can be described by [15]:

$$\alpha \propto \exp\left(\frac{E}{E_0}\right) \quad (2)$$

where E is the photo energy and $E_o$ is the characteristic slope also frequently called Urbach energy. The Urbach energy is determined to be around 124 meV as indicated in Fig. 3. The Urbach energy is related to the joint density-of-states determined by both conduction and valence band tail states. Because the valence-band-tail state can be broader (or shallower) than conduction-band-tail state, they dominate the optical absorption [16] and Urbach energy could be used to represent the valence-band-tail slope value. Such approximation had been commonly used in a-Si:H thin-film; and conduction-band-tail slope is usually about half of the valence-band-tail slope [17]. If we assume a similar situation to occur in a-IGZO, the valence-band-tail slope is approximately 124 meV and corresponding conduction-band-tail slope will be around 62 meV. Both values should be confirmed by other experimental methods.

### *3.2 Dark a-IGZO TFT Electrical Properties*

The output characteristics of the a-IGZO TFT under various gate voltages ($V_{GS}$) ranging from 4~20V are shown in Fig. 4(a). During each measurement, the drain voltage ($V_{DS}$) was varied from 0~20V. A very clear distinction between linear and saturation region is obtained. This suggests that less than 20V of drain voltage ($V_{DS}$) is adequate for operating a-IGZO TFT active-matrix arrays. The TFT source/drain property is another important aspect for TFT evaluation. A non-ohmic source/drain contact, improper active layer thickness (too thick) and high bulk density of states (DOS) can all cause TFT to have a non-linear drain current ($I_{DS}$)/ $V_{DS}$ behavior, also called "current crowding", at low $V_{DS}$ [18,19]. Fig. 4(b) shows the output characteristics near the origin ($V_{DS}$=0~1V) and there is no current crowding observed in a-IGZO TFT. The absence of current crowding can be better appreciated by plotting the derivative of the

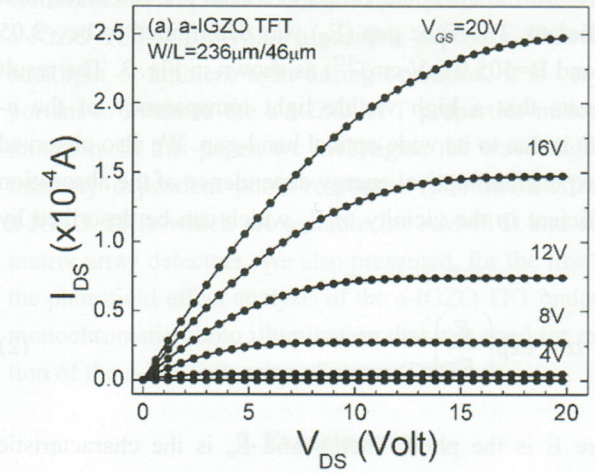


(a)

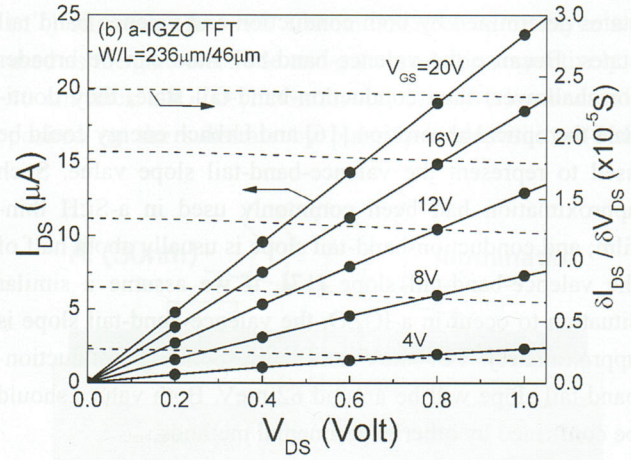


(b)

**Fig. 4.** (a) Output characteristics of PLD a-IGZO TFT. (b) A zoom-in plot of the output characteristic (solid curves) near the origin ($V_{DS}$=0~1V); the derivative of $I_{DS}$ vs. $V_{DS}$ characteristics ($\delta I_{DS}/\delta V_{DS}$, dash curved) are also shown. (Adapted from [28].)

output curves which is also shown in Fig. 4(b). These properties are highly desirable for a-IGZO TFT to be used in active-matrix arrays.

TFT dark transfer characteristics were also measured. Fig. 5(b) illustrates the saturation region ($V_{DS}$=12V) transfer characteristics of the a-IGZO TFT (W/L= 236μm/46μm). We extracted the threshold voltage ($V_{th}$) and field effect mobility ($\mu_{eff}$) based on the standard MOSFET equation:

$$I_{DS} = \mu_{eff} C_{ox} \frac{W}{2L} (V_{GS} - V_{th})^2 \qquad (3)$$

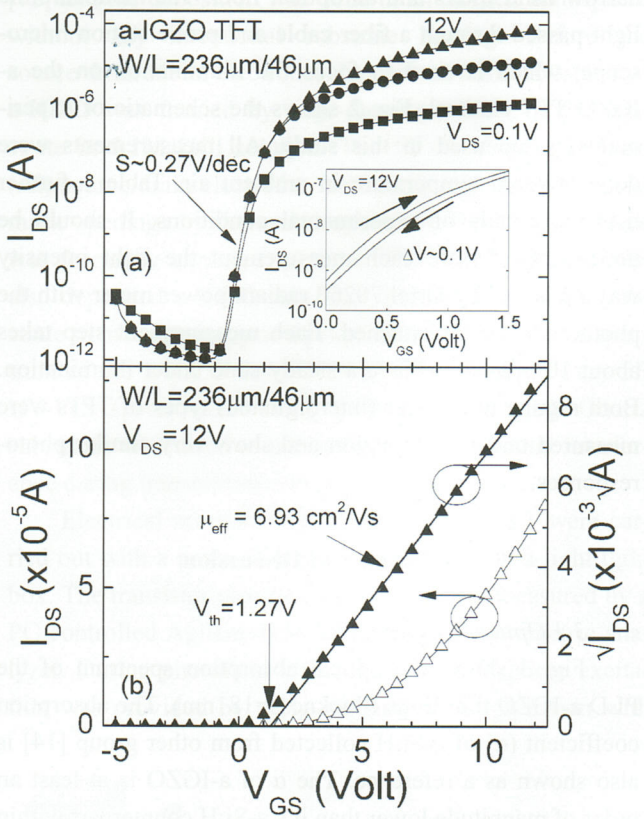


**Fig. 5.** Transfer characteristic of PLD a-IGZO TFT in (a) semi-log plot and (b) linear plot. (Inset, a) The TFT hysteresis measured at $V_{DS}$=12V; ΔV is the shift (hysteresis) in sub-threshold properties. (Adapted from [28].)

where $C_{ox}$ is the gate insulator capacitance per unit area, W and L are TFT channel width and length, respectively. The best linear fit of eq.(3) between 90% to 10% of the maximum $I_{DS}$ (at $V_{GS}$=12V) was found and the $V_{th}$ and $\mu_{eff}$ can be determined. The subthreshold swing (S) was also extracted from the subthreshold region data (Fig. 5(a)), using the following equation:

$$S = \left( \frac{d \log(I_{DS})}{dV_{GS}} \right)^{-1} \qquad (4)$$

Table 2 summarizes all key electrical properties for a-IGZO TFTs used in this study. The S for our a-IGZO TFTs is as low as 270 mV/dec. Such value is compatible or even superior to one obtained for a-Si:H TFT (0.3~0.4V/dec). This ensures a fast TFT response and also reduces the voltage of the gate driving signal. It should be noticed that higher $\mu_{eff}$ is observed for TFT with smaller W. Since these devices

**Table 2.** Key Electrical Properties of PLD a-IGZO TFTs Used in This Study

| TFT | | $\mu_{eff}$ | $V_{th}$ | S | $I_{DS\_off}$* | On/off |
|---|---|---|---|---|---|---|
| Type | Size (W/L) | ($cm^2$/Vs) | (V) | (V/dec.) | (A) | ratio* |
| Regular | 236μm/46μm | 6.93 | 1.27 | 0.27 | $10^{-12}$ | $10^8$ |
| | 1040μm/35μm | 3.2 | 2.8 | 0.28 | $<10^{-12}$ | $>10^8$ |
| Finger | 2811μm/26.5μm | 3.48 | 2.57 | 0.28 | $<10^{-12}$ | $>10^8$ |

* $I_{DS\_off}$ is the off-state drain-current and "on/off ratio" is the drain current ratio between on and off states.

have only macro-island patterned, channel current is not very well defined and could leak out near the channel edge. This phenomenon can cause an overestimation of $\mu_{eff}$ since the edge current could occupy significant portion of total drain current that is measured for TFT with smaller W. Such non-ideal effect has no direct impact on photofield-effect analysis described in this paper.

*3.3 Wavelength Dependent a-IGZO TFT Photo-Response*

The response of the PLD a-IGZO TFT to monochromatic illumination was studied by measuring the TFT transfer characteristic for various light wavelengths with a constant photon flux ($1\times10^{13}$ photons/$cm^2$s). Fig. 6 shows the a-IGZO TFT transfer characteristic in the dark and under illumination. We observed clearly a shift in TFT $I_{DS}$-$V_{GS}$ characteristics under illumination. Furthermore, a "threshold" wavelength exists when TFTs are illuminated: little or no shift occurs in TFT properties under illumination with $\lambda$>420nm (2.95eV) while a much larger change takes place when $\lambda$<420nm.

As shown in Fig. 6(a), the $I_{DS\text{-}off}$ of TFT under illumination increases significantly as the wavelength getting closer to UV region. Compared to the original dark condition, about three orders of magnitude increase occurs when we illuminated the device at $\lambda$=365nm (3.4eV). In contrast with $I_{DS\text{-}off}$, the $I_{DS\text{-}on}$ (drain current at $V_{DS}$=$V_{GS}$=12V) is rather constant. A negative shift in sub-threshold properties is also observed and the voltage shift about -7 volt was recorded for $\lambda$=365nm. Finally, the off-to-on switching in $I_{DS}$ becomes less steep when we illuminate the TFT at shorter wavelength. As consequence, the TFT subthreshold swing increases. Similar to the sub-threshold properties, in on-region, a negative shift of $V_{th}$ (Fig. 6(b)) is also observed.

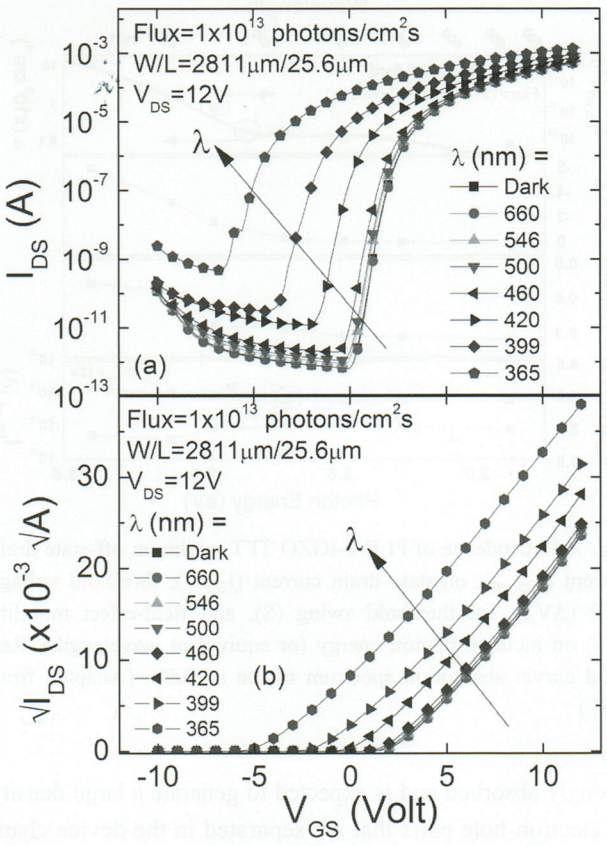


**Fig. 6.** PLD a-IGZO TFT transfer characteristics for constant photon flux with the varying illumination wavelengths. ((a): semi-log plot, (b): linear plot ; Adapted from [28].)

The threshold voltage shift ($\Delta V_{th}$=$V_{th\text{-}under\ illumination}$-$V_{th\text{-}in\ dark}$) was determined to be about -6V under illumination at $\lambda$=365nm. The slope of $\sqrt{I_{DS}}$-$V_{GS}$ shows almost no change within the wavelength range used in this study (Fig. 6(b)). This suggests the field-effect mobility ($\mu_{eff}$) is not affected by illumination. We further summarize the result by plotting various TFT parameters as a function of incident photon energy as shown in Fig. 7. After illumination, we can bring the device back to its original pre-illumination state by a $100^0$C thermal treatment for 3 minutes. With no applied heat, the device will regain its pre-illumination properties after a much longer period of time.

In the order to elucidate the physical origin of the change in TFT electrical properties, the a-IGZO absorption spectrum (red solid curve) is overlapped with the variation of the $I_{DS\_off}$ data in Fig. 7. It can be concluded that the light with energy less than 3.0 eV (visible region) is only weakly absorbed and has a negligible effect on the TFT transfer characteristics, while light with energy larger than 3.0 eV is

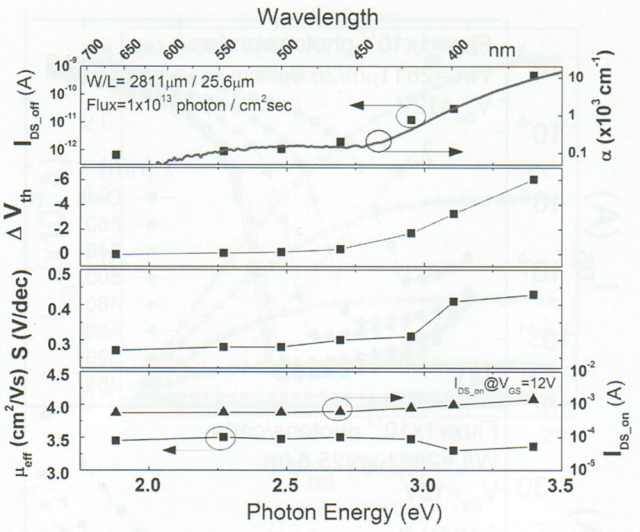


**Fig. 7.** Dependence of PLD a-IGZO TFT minimum off-state drain current ($I_{DS\_off}$), on-state drain current ($I_{DS\_on}$), threshold voltage shift ($\Delta V_{th}$), sub-threshold swing (S), and field-effect mobility ($\mu_{eff}$) on incident photon energy (or equivalent wavelength). Red solid curve: absorption spectrum of the a-IGZO. (Adapted from [28].)

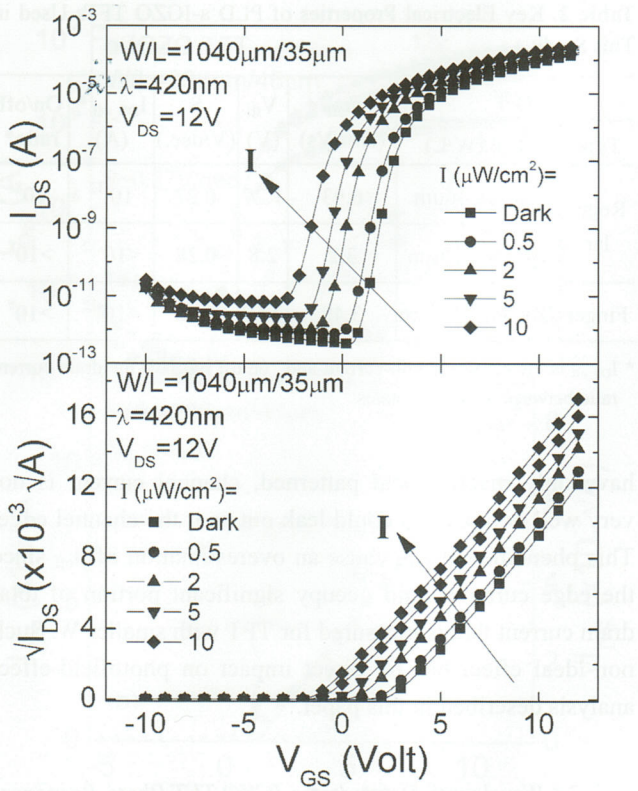


**Fig. 8.** PLD a-IGZO TFT transfer characteristics for dark and different irradiance levels (I) in (top): semi-log plot and (bottom) linear plot. (Adapted from [20].)

strongly absorbed and is expected to generate a large density of electron-hole pairs that are separated in the device channel by electrical field. During illumination, the threshold voltage ($V_{th}$) shifts to more negative $V_{GS}$ values with the increasing photo energy. We speculate that the positive charges are trapped (one possibility is hole trapping) within the channel or/and at the $SiO_2$ / a-IGZO interface and are responsible for the $\triangle V_{th}$. Also, the photogenerated electrons could appear to be more mobile than holes in TFT channel region. The exact nature of the traps is under present investigation.

*3.4 Intensity Dependent a-IGZO TFT Photo-Response*

To study the a-IGZO TFT response under different illumination intensity, we applied a UV monochromatic light ($\lambda$=420nm) to uniformly illuminate the TFT channel area directly through probe station microscope. The wavelength was chosen to match the absorption properties of the a-IGZO. At $\lambda$=420nm, our sample has absorption coefficient $\alpha \cong 714cm^{-1}$, which corresponds to an optical penetration depth ($\delta=1/\alpha$) of 14μm. Since $\delta$ is much larger than the thickness of the channel a-IGZO layer (40nm), the illumination is uniformly absorbed throughout the thickness during measurement. Fig. 8 shows the TFT transfer characteristics measured under dark and with different irradiance levels (I) up to $10\mu W/cm^2$. We further extracted TFT parameters for each individual level and plot them as a function of light intensity (Fig. 9). $I_{DS\_off}$ was found to increase with the illumination intensity, along with a negative shift of threshold voltage ($\Delta V_{th}$). S raises from 0.28 to 0.37 V/dec at $I=10\mu W/cm^2$. This is primarily due to the increase of $I_{DS\_off}$ as can clearly be seen when threshold voltage shift is used to normalize transfer curves (Fig. 10). The $\mu_{eff}$ almost remains unchanged during the illumination process. This result indicates a strong UV photon absorption in a-IGZO layer and electron-hole pairs generated by photo-excitation cause the bulk conductivity to increase. The observed negative $\Delta V_{th}$ is similar to what has been discussed in previous section. The photo-generated charge trapping is also occurring in this experiment. This can be further supported by the fact that all the TFT transfer curves share the same threshold voltage normalized turn-on voltage (about -2V) as illustrated in Fig. 10.

**Table 2.** Key Electrical Properties of PLD a-IGZO TFTs Used in This Study

| TFT | | $\mu_{eff}$ | $V_{th}$ | S | $I_{DS\_off}$* | On/off |
|---|---|---|---|---|---|---|
| Type | Size (W/L) | ($cm^2$/Vs) | (V) | (V/dec.) | (A) | ratio* |
| Regular | 236μm/46μm | 6.93 | 1.27 | 0.27 | $10^{-12}$ | $10^8$ |
| | 1040μm/35μm | 3.2 | 2.8 | 0.28 | $<10^{-12}$ | $>10^8$ |
| Finger | 2811μm/26.5μm | 3.48 | 2.57 | 0.28 | $<10^{-12}$ | $>10^8$ |

* $I_{DS\_off}$ is the off-state drain-current and "on/off ratio" is the drain current ratio between on and off states.

have only macro-island patterned, channel current is not very well defined and could leak out near the channel edge. This phenomenon can cause an overestimation of $\mu_{eff}$ since the edge current could occupy significant portion of total drain current that is measured for TFT with smaller W. Such non-ideal effect has no direct impact on photofield-effect analysis described in this paper.

*3.3 Wavelength Dependent a-IGZO TFT Photo-Response*

The response of the PLD a-IGZO TFT to monochromatic illumination was studied by measuring the TFT transfer characteristic for various light wavelengths with a constant photon flux ($1\times10^{13}$ photons/$cm^2$s). Fig. 6 shows the a-IGZO TFT transfer characteristic in the dark and under illumination. We observed clearly a shift in TFT $I_{DS}$-$V_{GS}$ characteristics under illumination. Furthermore, a "threshold" wavelength exists when TFTs are illuminated: little or no shift occurs in TFT properties under illumination with $\lambda$>420nm (2.95eV) while a much larger change takes place when $\lambda$<420nm.

As shown in Fig. 6(a), the $I_{DS\text{-}off}$ of TFT under illumination increases significantly as the wavelength getting closer to UV region. Compared to the original dark condition, about three orders of magnitude increase occurs when we illuminated the device at $\lambda$=365nm (3.4eV). In contrast with $I_{DS\text{-}off}$, the $I_{DS\text{-}on}$ (drain current at $V_{DS}$=$V_{GS}$=12V) is rather constant. A negative shift in sub-threshold properties is also observed and the voltage shift about -7 volt was recorded for $\lambda$=365nm. Finally, the off-to-on switching in $I_{DS}$ becomes less steep when we illuminate the TFT at shorter wavelength. As consequence, the TFT subthreshold swing increases. Similar to the sub-threshold properties, in on-region, a negative shift of $V_{th}$ (Fig. 6(b)) is also observed.

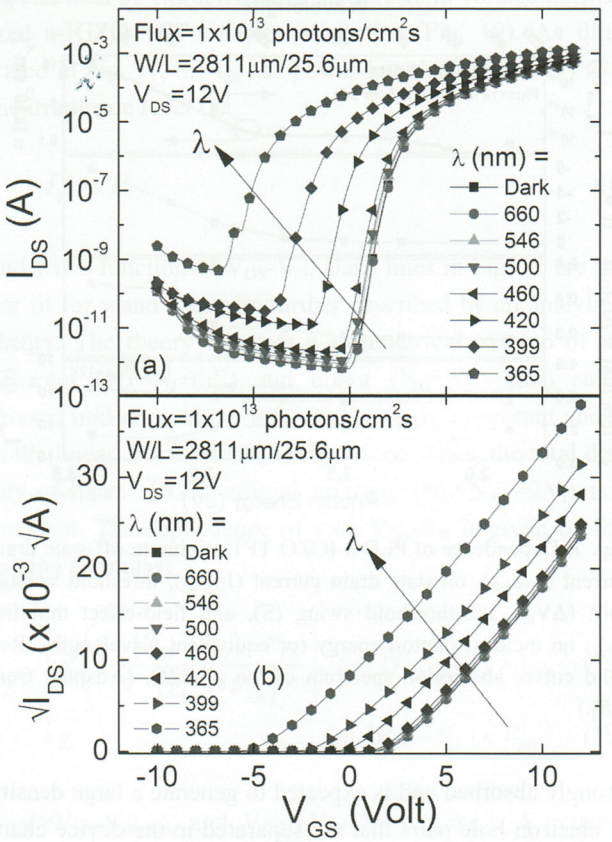


**Fig. 6.** PLD a-IGZO TFT transfer characteristics for constant photon flux with the varying illumination wavelengths. ((a): semi-log plot, (b): linear plot ; Adapted from [28].)

The threshold voltage shift ($\Delta V_{th}$=$V_{th\text{-}under\ illumination}$-$V_{th\text{-}in\ dark}$) was determined to be about -6V under illumination at $\lambda$=365nm. The slope of $\sqrt{I_{DS}}$-$V_{GS}$ shows almost no change within the wavelength range used in this study (Fig. 6(b)). This suggests the field-effect mobility ($\mu_{eff}$) is not affected by illumination. We further summarize the result by plotting various TFT parameters as a function of incident photon energy as shown in Fig. 7. After illumination, we can bring the device back to its original pre-illumination state by a $100^0$C thermal treatment for 3 minutes. With no applied heat, the device will regain its pre-illumination properties after a much longer period of time.

In the order to elucidate the physical origin of the change in TFT electrical properties, the a-IGZO absorption spectrum (red solid curve) is overlapped with the variation of the $I_{DS\_off}$ data in Fig. 7. It can be concluded that the light with energy less than 3.0 eV (visible region) is only weakly absorbed and has a negligible effect on the TFT transfer characteristics, while light with energy larger than 3.0 eV is

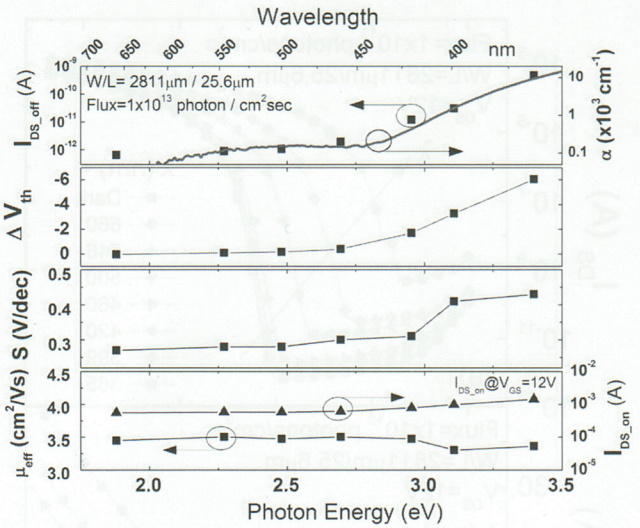


**Fig. 7.** Dependence of PLD a-IGZO TFT minimum off-state drain current ($I_{DS\_off}$), on-state drain current ($I_{DS\_on}$), threshold voltage shift ($\Delta V_{th}$), sub-threshold swing (S), and field-effect mobility ($\mu_{eff}$) on incident photon energy (or equivalent wavelength). Red solid curve: absorption spectrum of the a-IGZO. (Adapted from [28].)

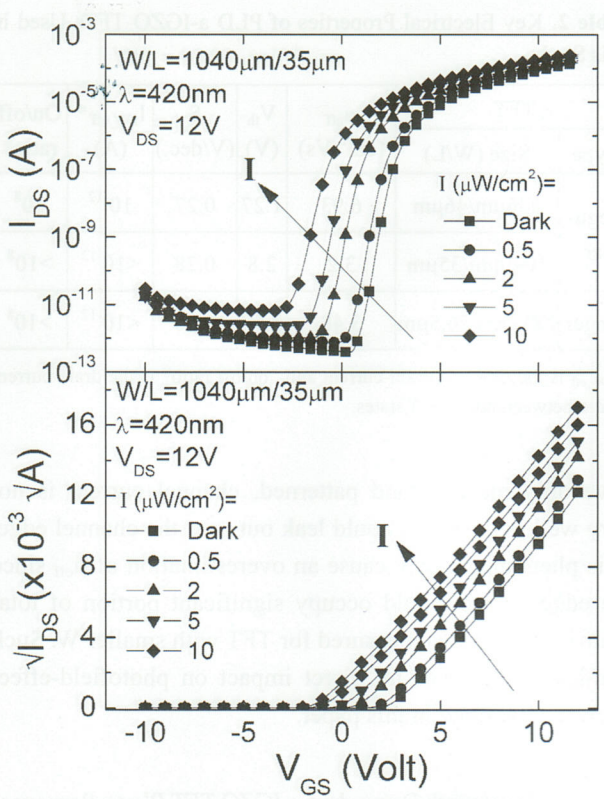


**Fig. 8.** PLD a-IGZO TFT transfer characteristics for dark and different irradiance levels (I) in (top): semi-log plot and (bottom) linear plot. (Adapted from [20].)

strongly absorbed and is expected to generate a large density of electron-hole pairs that are separated in the device channel by electrical field. During illumination, the threshold voltage ($V_{th}$) shifts to more negative $V_{GS}$ values with the increasing photo energy. We speculate that the positive charges are trapped (one possibility is hole trapping) within the channel or/and at the $SiO_2$ / a-IGZO interface and are responsible for the $\triangle V_{th}$. Also, the photogenerated electrons could appear to be more mobile than holes in TFT channel region. The exact nature of the traps is under present investigation.

*3.4 Intensity Dependent a-IGZO TFT Photo-Response*

To study the a-IGZO TFT response under different illumination intensity, we applied a UV monochromatic light ($\lambda$=420nm) to uniformly illuminate the TFT channel area directly through probe station microscope. The wavelength was chosen to match the absorption properties of the a-IGZO. At $\lambda$=420nm, our sample has absorption coefficient $\alpha \cong 714cm^{-1}$, which corresponds to an optical penetration depth ($\delta=1/\alpha$) of 14μm. Since $\delta$ is much larger than the thickness of the channel a-IGZO layer (40nm), the illumination is uniformly absorbed throughout the thickness during measurement. Fig. 8 shows the TFT transfer characteristics measured under dark and with different irradiance levels (I) up to $10\mu W/cm^2$. We further extracted TFT parameters for each individual level and plot them as a function of light intensity (Fig. 9). $I_{DS\_off}$ was found to increase with the illumination intensity, along with a negative shift of threshold voltage ($\Delta V_{th}$). S raises from 0.28 to 0.37 V/dec at $I=10\mu W/cm^2$. This is primarily due to the increase of $I_{DS\_off}$ as can clearly be seen when threshold voltage shift is used to normalize transfer curves (Fig. 10). The $\mu_{eff}$ almost remains unchanged during the illumination process. This result indicates a strong UV photon absorption in a-IGZO layer and electron-hole pairs generated by photo-excitation cause the bulk conductivity to increase. The observed negative $\Delta V_{th}$ is similar to what has been discussed in previous section. The photo-generated charge trapping is also occurring in this experiment. This can be further supported by the fact that all the TFT transfer curves share the same threshold voltage normalized turn-on voltage (about -2V) as illustrated in Fig. 10.

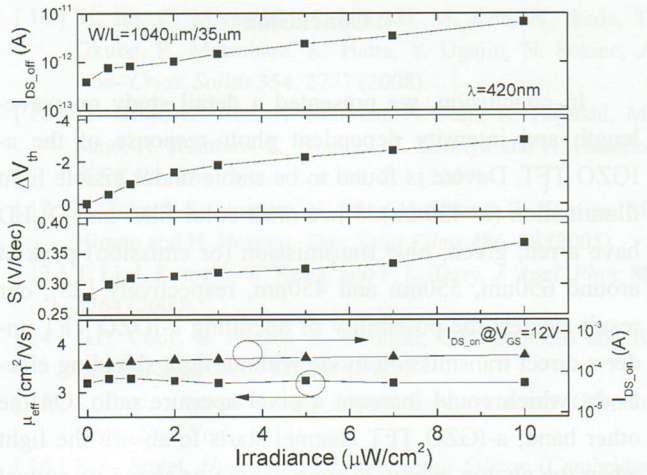


**Fig. 9.** Dependence of PLD a-IGZO TFT $I_{DS\_off}$, on-state drain current ($I_{DS\_on}$), $\Delta V_{th}$, S, and $\mu_{eff}$ on irradiance level. (From [20].)

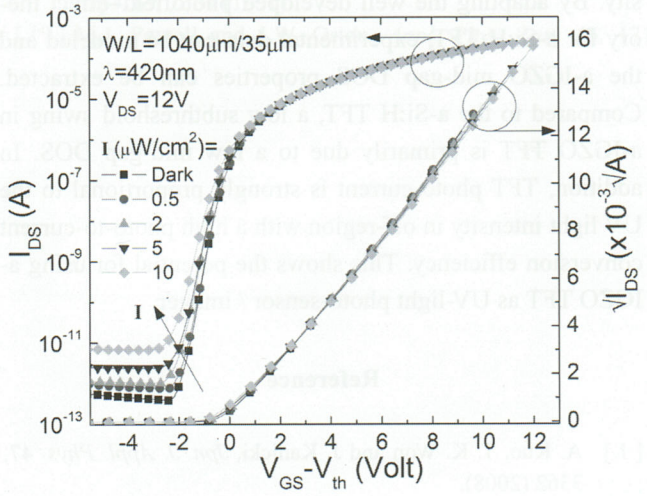


**Fig. 10.** Threshold voltage normalized ($I_{DS}$ is plotted as a function of effective gate voltage, $V_{GS}$-$V_{th}$) PLD a-IGZO TFT transfer properties for dark and different irradiance levels (I). (From [20].)

### *3.5 Photofield-Effect Analysis [20]*

The photofield-effect theory was originally developed by Schropp *et al.* and later used to explain the photoconductivity under a controlled gate bias in a-Si:H TFT [21-23]. It was also successfully used to analyze the electrical properties under illumination in organic polymer TFT [24]. The analysis begins with the definition of photo-current ($I_{ph}$) as the difference between TFT drain current under illumination and dark:

$$I_{ph} = I_{DS\_ill} - I_{DS\_dark} \tag{5}$$

$I_{ph}$ can then be extracted from the threshold voltage normalized a-IGZO TFT transfer properties (Fig. 10). As illustrated in Fig. 11, the $I_{ph}$ has power-law dependence ($\gamma$) with the irradiance level (I):

$$I_{ph} \propto I^{\gamma} \tag{6}$$

and $\gamma$ is a function of $V_{GS}$-$V_{th}$. Dash lines in Fig. 11 are linear fit for $\gamma$ and it can be further described by an analytical theory. The theory assumes a symmetrical overlap of the acceptor ($N_A$=$N_f$+mE) and donor ($N_D$=$N_f$ - mE) states around mid-gap, where E is energy, $N_f$ is a constant and m is the linear characteristic energy slope. Thus, the total density-of-states (DOS) around mid-gap ($N_D$+$N_A$ =2$N_f$) is a constant. The dependence of $\gamma$ on $V_{GS}$-$V_{th}$ is given by following formulas:

$$\gamma = \begin{cases} \gamma_0 \left( 1 - \dfrac{(V_{GS} - V_{th}) - V_{FB}'}{(V_{GC}' - V_{FB}')} \right), & for\ (V_{GS} - V_{th}) > V_{FB}' \quad (7a) \\ \gamma_0, & for\ (V_{GS} - V_{th}) < V_{FB}' \quad (7b) \end{cases}$$

$V_{FB}'$=$V_{FB}$-$V_{th\_dark}$ and $V_{GC}'$=$V_{GC}$-$V_{th\_dark}$. $\gamma_0$ is a material dependent constant. $V_{FB}$ and $V_{th\_dark}$ are flat band voltage and dark threshold voltage, respectively. $V_{GC}$ is also called critical voltage and is defined as:

$$V_{GC} = \frac{d_{ins}}{\varepsilon_{ins}} \left( \frac{\varepsilon_{semi}}{\varepsilon_0} \right)^{1/2} \frac{(2N_f)^{3/2}}{m} \tag{8}$$

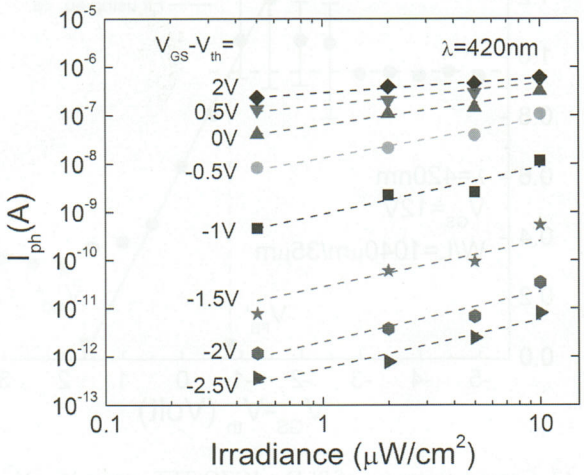


**Fig. 11.** Dependence of photocurrent ($I_{ph}$) on irradiance at various $V_{GS}$-$V_{th}$ voltages. Dash lines are linear fits for power-law dependence coefficients gamma ($\gamma$). (From [20].)

where $d_{ins}$ is the gate insulator thickness (=100nm), $\varepsilon_{ins}$ and $\varepsilon_{semi}$ are dielectric constants for gate insulator (3.9 for $SiO_2$) and a-IGZO (=10), respectively. Fig. 12 shows the $\gamma$ extracted from Fig. 11 as a function of $V_{GS}$-$V_{th}$ and the experimental data closely follow the analytical model (eq.7). The $\gamma_0$ is extracted to be near 1.0 which indicates that a-IGZO TFT is efficiently converting the UV-illumination to photocurrent in off-region. We then extracted the critical voltage ($V_{GC}$) and flat-band voltage ($V_{FB}$) to be 4.44V and 1.99V, respectively. In order to determine the mid-gap DOS characteristic slope m, we first determined the total mid-gap DOS, $2N_f$, by using the following formula [25]:

$$2N_f = \left( \frac{S \log(e)}{kT/q} - 1 \right) \frac{C_{ox}}{q} \tag{9}$$

where S is the TFT subthreshold swing. The $2N_f$ for our a-IGZO TFT is estimated to be ~$10^{17}$ $cm^{-3}eV^{-1}$ which is consistent with the value (< $4\times10^{17}$ $cm^{-3}eV^{-1}$) extracted using SPICE modeling [26]. By substituting all the parameters into eq.8, m is calculated to be $7.76\times10^{16}$ $cm^{-3}eV^{-2}$. The extracted a-IGZO TFT mid-gap DOS is more than a order lower than the previously reported values for a-Si:H TFT [27]. This finding is supporting a good switching property of the a-IGZO TFTs that was experimentally observed by different laboratories across world.

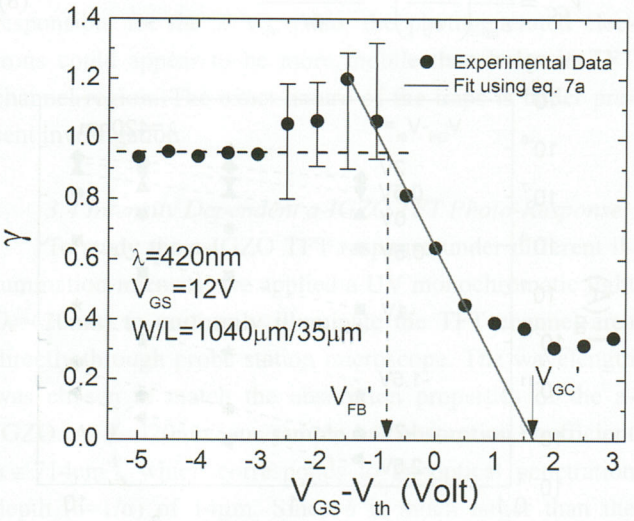


**Fig. 12**. Gamma factor ($\gamma$) of PLD a-IGZO TFT versus $V_{GS}$-$V_{th}$ at a wavelength of 420nm. (From [20].)

## 4. Conclusion

In conclusion, we presented a detail study on wavelength and intensity dependent photo-response of the a-IGZO TFT. Device is found to be stable under visible light illumination ($\lambda$>420nm). Since most color filter and OLED have a red, green, blue transmission (or emission) peak at around 650nm, 550nm and 450nm, respectively [28], our result suggest the possibility of operating a-IGZO TFT under a direct transmission mode without light shielding electrode, which could increase a pixel aperture ratio. On the other hand, a-IGZO TFT channel starts to absorb the light when the photon energy is approaching or above its optical band gap (~3eV, near UV region) and the $I_{DS\_off}$ increases along with a negative shift of $V_{th}$. The increase of $I_{DS\_off}$ is also found to be proportional to the UV illumination intensity. By adapting the well developed photofield–effect theory for a-Si:H TFT, experimental data can be modeled and the a-IGZO mid-gap DOS properties can be extracted. Compared to the a-Si:H TFT, a low subthreshold swing in a-IGZO TFT is primarily due to a low mid-gap DOS. In addition, TFT photo-current is strongly proportional to the UV light intensity in off-region with a high photo-to-current conversion efficiency. This shows the potential for using a-IGZO TFT as UV-light photo-sensor / imager.

## Reference


[1] A. Kuo, T. K. Won and J. Kanicki, *Jpn. J. Appl. Phys.* **47**, 3362 (2008).

[2] J.K. Jeong, H.-J. Chung, Y.-G. Mo and H.D. Kim, *Information Display* **9**, 20 (2008)

[3] T. Sameshima, S. Usui and M. Sekiya, *IEEE Electron Device Lett.* **7**, 276 (1986).

[4] S. S. Kim, B. H. You, J. H. Cho, S. J. Moon, B. H. Berkeley and N.D. Kim, in *SID Int. Symp. Digest (2008)*, p. 196.

[5] R.A. Street and L.E. Antonuk, *IEEE Circuit and Device Magazine* **9**, 39 (1993).

[6] H. Hosono, *J. Non- Cryst. Solids* **352**, 851 (2006).

[7] K. Nomura, H. Ohta, A. Takagi, T. Kamiya, M. Hirano and H. Hosono, *Nature* **432**, 488 (2004).

[8] J. K. Jeong, J. H. Jeong, J. H. Choi, J. S. Im, S. H. Kim, H. W. Yang, K. N. Kang, K. S. Kim, T. K. Ahn, H.-J. Chung, M. Kim, B. S. Gu, J.-S. Park, Y.-G. Mo, H. D. Kim and H. K. Chung, *SID Int. Symp. Digest (2008)*, p. 1.

[9] J.-H. Lee, D.-H Kim, D.-J. Yang, S.-Y. Hong, K.-S. Yoon, P.-S. Hong, C.-O Jeong, H.-S. Park, S.-Y. Kim, S.-K. Lim and S.-S. Kim, *SID Int. Symp. Digest (2008)*, p. 625.

[ 10 ] M. Ito, C. Miyazaki, M. Ishizaki, M. Kon, N. Ikeda, T. Okubo, R. Matsubara, K. Hatta, Y. Ugajin, N. Sekine, *J. Non- Cryst. Solids* **354**, 2777 (2008).

[ 11 ] M. Ofuji, K. Abe, H. Shimizu, N. Kaji, R. Hayashi, M. Sano, H. Kumomi, K. Nomura, T. Kamiya and H. Hosono, *IEEE Electron Device Lett.* **28**, 273 (2007).

[ 12 ] A. Takagi, K. Nomura, H. Ohta, H. Yanagi, T. Kamiya, M. Hirano and H. Hosono, *Thin Solid Films* **486**, 38 (2005).

[ 13 ] T. Li, J. Kanicki, W. Kong, and F. L. Terry, *J. Appl. Phys.* **88**, 5764 (2000).

[ 14 ] G.D. Cody, B. Abeles, C. Wronski, C.R. Stephens and B. Brooks, *Solar Cells* **12**, 221 (1985).

[ 15 ] J. Tauc, *Amorphous and Liquid Semiconductors* (Plenum Press, New York, 1974)

[ 16 ] R.A. Street, *Hydrogenated Amorphous Silicon* (Cambridge University Press, New York, 1991), p.88.

[ 17 ] S. Sherman, S. Wagner, R. A. Gottscho, *Appl. Phys. Lett.* **69**, 3242 (1996).

[ 18 ] J. Kanicki, F.R. Libsch, J. Griffith and R. Polastre, *J. Appl. Phys.* **69**, 2339 (1991).

[ 19 ] M.J. Powell and J.W. Orton, *Appl. Phys. Lett.* **45**, 171 (1984).

[ 20 ] T.-C. Fung, C.-S. Chuang, B G. Mullins, K. Nomura, T. Kamiya, H.-P.D. Shieh, H. Hosono and J. Kanicki, *IMID Digest (2008),* p.1208.

[ 21 ] R.E.I. Schropp, G.J.M. Brouwer and J.F. Verwey, *J. Non-Cryst. Solids,* **77&78**, 511 (1985).

[ 22 ] R.E.I. Schropp, T. Franke and J.F. Verwey, *J. Non- Cryst. Solids* **90**, 199 (1987).

[ 23 ] J.D. Gallezot, S. Martin and J. Kanicki, *Proc. IDRC* (2001), p. 407.

[ 24 ] M.C. Hamilton and J. Kanicki, *IEEE J. Select. Topics Quantum Electron.* **10**, 840 (2004).

[ 25 ] A. Rolland, J. Richard, J.-P. Kleider and D. Mencaraglia, *J. Electrochem. Soc.* **140**, 3679 (1993).

[ 26 ] C. Chen, T.-C. Fung, K. Abe, H. Kumomi and J. Kanicki, *Proceeding of 66th Device Research Conference* (2008), p. 151.

[ 27 ] A. O. Harm, R.E.I. Schropp and J. F. Verwey, *Phil. Mag. B* **52**, 59 (1985).

[ 28 ] C.-S. Chuang, T.-C. Fung, B G. Mullins, K. Nomura, T. Kamiya, H.-P.D. Shieh, H. Hosono and J. Kanicki, *SID Int. Symp. Digest (2008),* p.1215.

※ Parts of this work were presented in Proceedings of IMID 2008